PHYSICAL REVIEW B VOLUME 23, NUMBER 4 15 FEBRUARY 1981

Local electronic structure of amorphous metal alloys using cluster models. Evidence for specific metalloid-metal interactions

R. P. Messmer
General Electric Corporate Research and Development, Schenectady, New York 12301
(Received 21 July 1980)

Although considerable effort has been expended over the past ten years on constructing structural models of amorphous metal alloys, mostly through the application of "dense random packing of hard spheres" ideas and extensions thereof, almost no theoretical effort has been devoted to understanding the local electronic structure and chemical interactions among the various components in such alloys. The present work is part of a substantial effort which is being made to rectify this situation. Detailed quantum-mechanical calculations are carried out on clusters of atoms which simulate possible local environments in amorphous metal alloys. The clusters used are based on simple Bernal polyhedra and distortions of these polyhedra. The materials being studied are the (Fe, Ni, B, P) alloys. In this paper, the simplest Bernal polyhedron, the tetrahedron, is considered as a first model for the local environment in $Fe_{40}Ni_{40}B_{20}$ and $Fe_{40}Ni_{40}P_{20}$ alloys. The tetrahedron contains two Fe atoms and two Ni atoms at the vertices with either a B atom or a P atom at the center. Spin-polarized self-consistent-field–$X\alpha$–scattered-wave calculations have been employed to investigate the electronic structure. It is found that there are considerable bonding interactions between the metalloid atoms (B or P) and the metal atoms of the clusters. Furthermore a detailed analysis of the charge densities of these models leads to the conclusion that the B atom should have a stronger interaction with the Ni atoms than with the Fe atoms, whereas the P atom should have a stronger interaction with the Fe atoms than with the Ni atoms. A brief discussion of recent experimental data which supports this conclusion is presented.

I. INTRODUCTION

Considerable evidence has been accumulated over the last few years pointing to the existence of definite chemical bonding effects between the metalloid atoms (M) and the transition-metal atoms (T) in amorphous alloys of the form $T_{100-x}M_x$. For example, just recently such evidence has been obtained from such disparate sources as x-ray photoelectron spectroscopy of the valence-band region of amorphous Fe-B alloy,[1] numerical calculations on the structure of binary T-M alloys using dense random packing of hard spheres (DRPHS) and relaxed models,[2] and the correlation of density measurements with other physical properties for ternary alloys of the form $(T_{100-Y}T'_Y)_{100-x}M_x$ with T = Mo, W, Ru and M = B, Si, P.[3]

Such results clearly indicate the need for understanding the nature of these chemical interactions at a very fundamental level in order to determine the degree to which the various observed properties follow as a consequence of chemical-bonding effects. The most fundamental approach is to study the electronic structure of such systems from a fully quantum-mechanical viewpoint. However, this is clearly impossible at the outset for such a complicated system as an amorphous metal if we wish to retain any rigorous theoretical approach. Thus we must be willing to accept what at first sight might appear to be rather severe approximations in order to make any progress on the problem. The details of the approximations will depend on which aspects of the electronic structure we wish to focus.

For those aspects of the electronic structure of interest in this study, namely, the chemical-bonding aspects, a model which focuses on the bonding between a metalloid atom and its local metal environment would appear to be most suitable. Within this context electronic-structure calculations on clusters of atoms which simulate the local environment about a metalloid atom should yield valuable information. However, the obvious problem for amorphous materials is the exact nature of the local environment, i.e., how does one choose the coordinates of the atoms in the cluster?

For the case of metal-metalloid amorphous alloys there appears to be a general consensus that the Bernal polyhedra offer a useful first approximation to the local atomic arrangement. In the alloys of interest here, it will be assumed that a B or P atom resides in the interstitial hole of a Bernal polyhedron. This seems reasonable as the size of these atoms is considerably smaller than a transition-metal atom and further the polyhedron might relax to better accommodate such a metalloid atom. In this paper only the smallest Bernal polyhedron, the tetrahedron, will be considered in any detail, even though other polyhedra may constitute more appropriate local environments for a metalloid atom. It is clear that a variety of local environments must be

explored in order to arrive at a perspective which one could consider to be general. However, the reason for the initial focus on the tetrahedron is simply that a number of important conceptual and computational questions can be addressed with a minimum of computational time and expense. The most important question for this work is whether there is theoretical evidence for significant bonding between metalloid and metal atoms, and if there is, to elucidate the nature of the bonding.

It should be mentioned that previous work which has employed molecular-orbital electronic-structure calculations in conjunction with clusters of atoms representing a local region of a solid has provided unique insight into a number of problems: These include defects in semiconductors,[4] chemisorption,[5] magnetic impurities in metals,[6] and impurities at grain boundaries.[7]

II. RESULTS FOR TETRAHEDRAL CLUSTERS

The results of calculations on three tetrahedral clusters will be discussed. These clusters are Ni_2Fe_2, Ni_2Fe_2B, and Ni_2Fe_2P, which are primitive models for the alloys $Ni_{50}Fe_{50}$, $Ni_{40}Fe_{40}B_{20}$, and $Ni_{40}Fe_{40}P_{20}$, respectively. If one chooses a metal-metal distance for the clusters appropriate to bulk Ni or Fe, the metal-metalloid distance found is 1.53 Å, which is too short. Hence the cluster was expanded to give a metal-metalloid distance of 2.13 Å, which is more consistent with known distances in the crystalline compounds Fe_3P and Ni_3B.[8] Only the results of the clusters with the larger metal-metalloid distance will be discussed in detail, although calculations on Ni_2Fe_2 and Ni_2Fe_2B clusters at the shorter distance were also carried out and will be briefly mentioned.

In Fig. 1, the geometry of the cluster is shown together with the coordinate system which will be used to discuss the results. The Ni atoms are contained in the yz plane and the Fe atoms in the xz plane. The electronic-structure calculations employed the self-consistent-field-$X\alpha$-scattered-wave (SCF-$X\alpha$-SW) method which has been described in detail in the literature[9] and which has been previously applied to a variety of problems involving metal clusters.[5-7,10,11] The present calculations have been carried out within the the spin-polarized framework in order to account for the magnetic effects of Fe-Ni clusters. Some details of the computations are discussed in the Appendix.

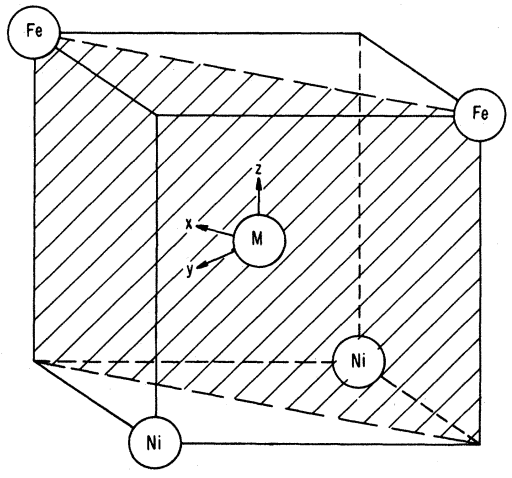

FIG. 1. Cluster geometry and coordinate system used for the Ni_2Fe_2M clusters.

In Fig. 2, the calculated valence orbital energy levels of the Ni_2Fe_2 cluster are presented. The majority spin orbitals (spin up) and minority spin orbitals (spin down) are shown separately. The levels denoted by solid lines each contain one electron; those denoted by dashed lines are unoccupied. The molecular-orbital levels are labeled according to the irreducible representations of the C_{2v} point group under which their corresponding orbital wave functions transform. Groups of levels which are primarily associated with Fe or Ni, i.e., whose wave functions are primarily on the Fe or Ni atoms, respectively, are indicated in the figure. From the figure it can

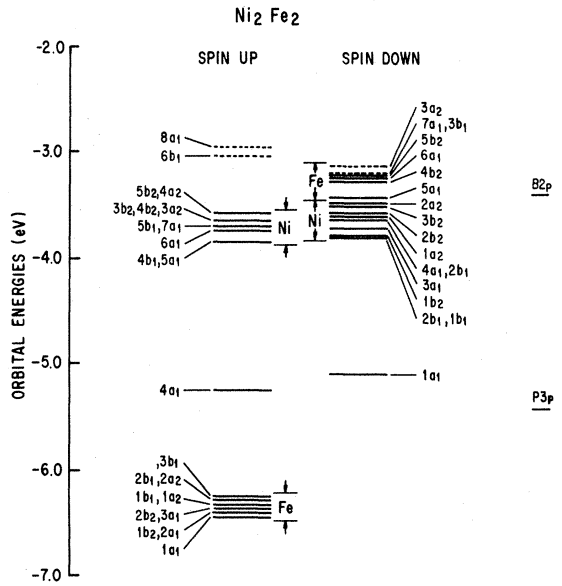

FIG. 2. Ni_2Fe_2 orbital energy-level diagram from SCF-$X\alpha$-SW spin-polarized calculation. Solid lines denote occupied orbitals, dashed lines are unoccupied. Groups of levels whose corresponding molecular orbitals are largely localized on one type of metal atom are denoted. The atomic B $2p$ and P $3p$ levels are shown at the right.

be seen that there is a large spin polarization associated with the Fe (i.e., a large splitting of the spin-up and spin-down Fe levels) and only a small spin polarization of the Ni levels.

The number of effective ferromagnetic electrons per metal atom is given by $(n^{\uparrow} - n^{\downarrow})/N = n_e$, where $n^{\uparrow}$ and $n^{\downarrow}$ are the number of spin-up and spin-down electrons, respectively (see Fig. 2), and N is the number of metal atoms. The quantity n_e is related to the saturation magnetization at 0 K by $M_s(0) = \mathfrak{N}\frac{1}{2} r g n_e \mu_B = \mathfrak{N} n_B \mu_B$ where μ_B is the Bohr magneton, the g factor accounts for orbital contributions, and $\mathfrak{N}$ is the number of magnetic atoms per unit volume; n_B is referred to as the effective magneton number. For the Ni_2Fe_2 cluster, the calculation yields a value of $n_B = 1.65$ which is the same as that of the bulk alloy $Ni_{50}Fe_{50}$.[12] Such close agreement is clearly accidental in this case, although one might hope that such calculations for the series, Ni_2Fe_2, Ni_2Fe_2B, and Ni_2Fe_2P would give a reasonable trend when compared to experiment; this is discussed below. The calculated value of n_B for the smaller metal–metal distance (i.e., 2.49 Å) is also 1.65.

Figure 3 shows the orbital energy levels which arise from a calculation for the Ni_2Fe_2B cluster. Again the levels which are predominantly Ni or Fe in the content of their wave functions are so labeled. Note that the effect of the B atom is to spread out the levels as compared to those in Fig. 2, where they are rather bunched together. It should also be noted that the Ni levels are more spread out in energy than the Fe levels as a consequence of the interaction with the B atom. This suggests that the B may be interacting more strongly with the Ni atoms than with the Fe atoms, an effect which will be discussed later. Two valence levels are not shown in Fig. 3; they are the $1a_1^{\uparrow}$ and $1a_1^{\downarrow}$ levels which occur at −11.0 and −10.6 eV, respectively. These levels correspond to the 2s level of B with a small admixture of Ni and Fe 4s and 3d character.

The B 2p orbitals interact significantly with the metal d orbitals and are responsible for lowering the $5a_1^{\uparrow}$, $4b_1^{\uparrow}$, $3b_2^{\uparrow}$, $1b_2^{\downarrow}$, $2a_1^{\downarrow}$, and $1b_1^{\downarrow}$ orbitals in Fig. 3 as compared to their position in Fig. 2. In Fig. 4, contour plots of the $1a_1^{\uparrow}$ and $5a_1^{\uparrow}$ orbitals are shown, from which it can be seen that the $1a_1^{\uparrow}$ level is predominantly B 2s although there is a small bonding interaction with the Fe atoms [see panel 4(b)], while the $5a_1^{\uparrow}$ orbital shows a bonding interaction between the B 2p_z and the Ni d orbitals and a nonbonding or slightly antibonding interaction with the Fe atoms. The other orbitals with significant B 2p character (noted

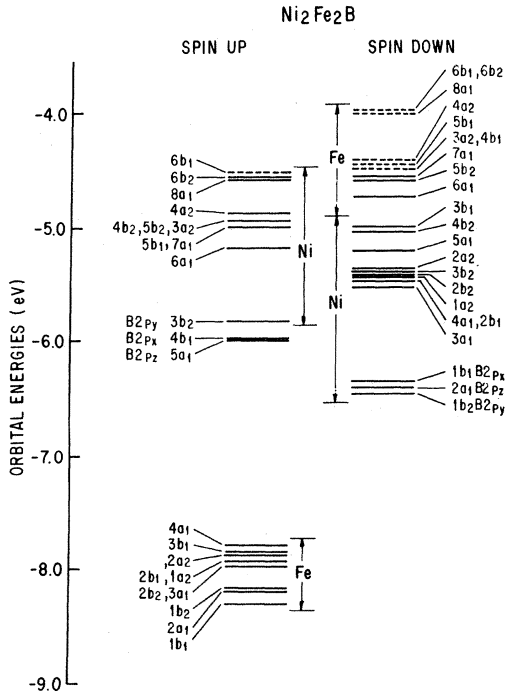

FIG. 3. Ni_2Fe_2B orbital energy-level diagram analogous to Fig. 2. The levels which have orbitals containing significant B content are labeled. Note the large spread of the Ni-like levels as compared to Fig. 2.

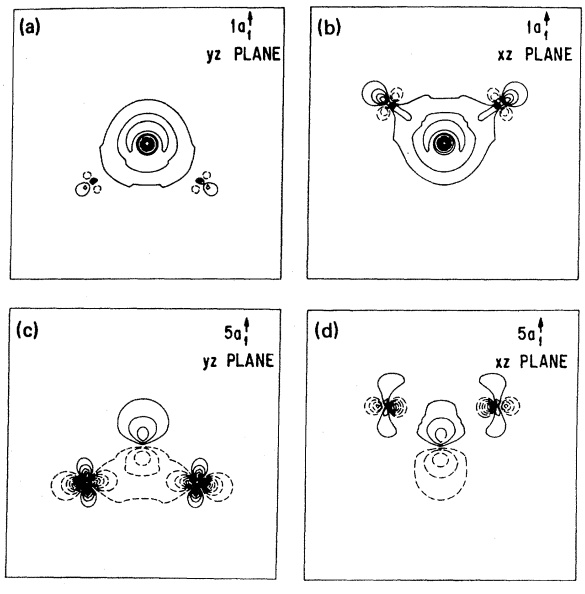

FIG. 4. Orbital contour plots of the $1a_1^{\uparrow}$ and $5a_1^{\uparrow}$ orbitals of Ni_2Fe_2B. The $1a_1^{\uparrow}$ orbitals are predominantly of B 2s character. The yz plane shows the interaction of B with the Ni atoms. The xz plane shows the interaction of B with the Fe atoms. (See Fig. 1.) The contour values for all the orbitals shown in this paper start at 0.05 a.u. and increase in units of 0.05 a.u.

in Fig. 3) also have bonding interactions with the metal atoms.

The highest occupied levels for Ni_2Fe_2B are the $6b_2^{\uparrow}$ and $7a_1^{\downarrow}$ which have the same energy and an occupancy of 0.6 and 0.4, respectively. For this case $n_B = 1.71$. No SCF solution was found which had integral occupation numbers and simultaneously satisfied Fermi statistics. The integral occupation number solution, which is very close to the level diagram of Fig. 3, has the $6b_2^{\uparrow}$ level empty and the $7a_1^{\downarrow}$ containing one electron with the $6b_2^{\uparrow}$ level at a slightly lower energy (0.15 eV) than the $7a_1^{\downarrow}$ level (i.e., Fermi statistics are not satisfied). To determine reliably such small differences in energy levels is beyond the inherent accuracy of the calculations and thus one cannot really decide which is the more appropriate solution. Fortunately, as far as the chemical-bonding aspects are concerned, the two solutions are virtually identical. The only significant difference is clearly in the calculation of the magnetic moment which depends very sensitively on the change in occupancy from 0.6 electron in a spin-up orbital and 0.4 electron in a spin-down orbital to one electron in a spin-down orbital. Thus the value of $n_B = 1.38$ is obtained for the integral occupation case. These values of n_B may be compared to the experimental value of 1.31 for the $Ni_{40}Fe_{40}B_{20}$ amorphous alloy.[13] The calculated value of n_B for the short T–M distance of 1.53 Å is 0.83.

Figure 5 shows the computed orbital energy-level diagram for the Ni_2Fe_2P cluster. Again the energy levels are labeled according to their dominant metallic character. The $1a_1^{\uparrow}$ and $1a_1^{\downarrow}$ levels are not shown in the figure; they are situated at −11.81 and −11.86 eV, respectively. These levels correspond to virtually pure atomic P 3s orbitals, as can be seen from Fig. 6. There are three levels which contain predominantly P 3p character; these are the $1b_2^{\uparrow}$, $1b_1^{\downarrow}$, and $2a_1^{\downarrow}$ orbitals (see Fig. 5). The P interaction with the metal atoms appears to be much more ionic in character than for the case of B, i.e., the orbitals of Fig. 6 are more heavily weighted on the P atom than those of Fig. 4 are on the B atom. There are nonetheless definite bonding interactions between the P 3p orbitals and the metal atoms. The calculated value of n_B is 0.83, which may be compared to the experimental value of 1.08 for the $Ni_{40}Fe_{40}P_{20}$ amorphous alloy.[13] For the case of the Ni_2Fe_2P cluster there are no problems with noninteger occupation numbers such as those found for the Ni_2Fe_2B cluster. It should be emphasized again that the calculated values of n_B for such small culsters cannot be expected to be very accurate. The change of one majority spin

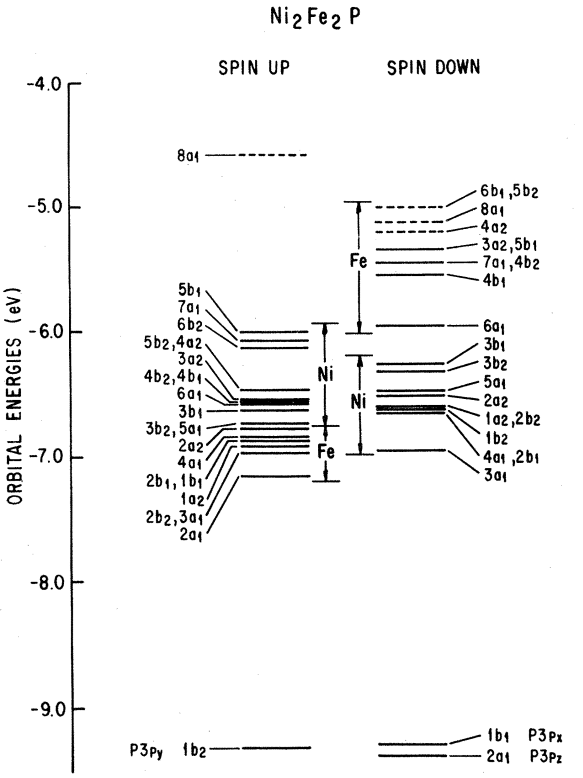

FIG. 5. Ni_2Fe_2P orbital energy-level diagram analogous to Figs. 2 and 3. The levels whose orbitals contain significant P content are labeled.

electron to a minority spin orbital (or vice versa) will change the calculated value of n_B by 0.55. It is thus rather amazing that the calculated values of n_B provide a reasonable trend when compared to experiment. This is summarized in Table I.

III. DISCUSSION

From the results in the last section, it is clear that there are significant bonding interactions between the p orbitals of B and P atoms and the atomic orbitals of the transition-metal atoms. One interesting question which comes to mind with regard to analyzing these results is whether there is a preferential interaction between a given metalloid atom and the Fe or Ni atoms in the cluster. If such preferential interactions do occur they would have a profound effect on the conceptual framework with which we view metalloid–transition-metal glasses. For T-T'-M systems, one could no longer view the metalloid atoms as simply filling in the Bernal holes of a DRPHS structure of metal atoms. Rather, one would have to admit to the possibility of a *local atomic scale chemistry* arising from such electronic interactions.

In analyzing the results of the simple clusters

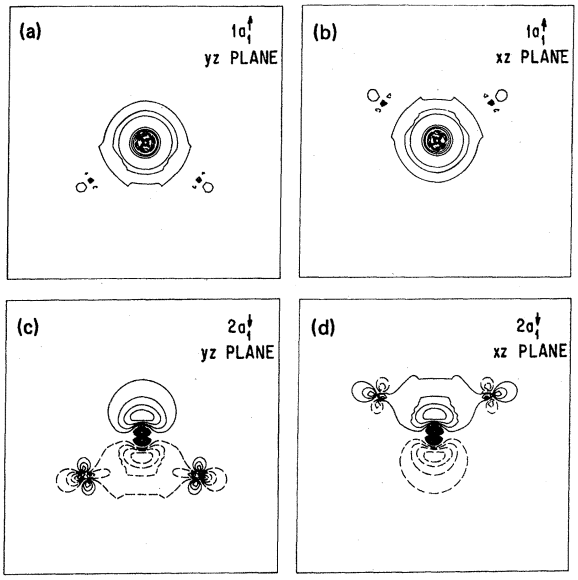

FIG. 6. Orbital contour plots of the $1a_1^\uparrow$ and $2a_1^\uparrow$ orbitals of Ni_2Fe_2P. The $1a_1^\uparrow$ is almost pure P 2*s*. The *yz* plane shows the interaction of P with the Ni atoms. The *xz* plane shows the interaction of P with the Fe atoms (see Fig. 1). The contour values are as in Fig. 4.

considered in this work, it must be kept in mind that they can only give a clue as to the nature of the local chemistry. Much more work will have to be done on larger clusters and on differing local environments to completely elucidate the local chemistry. However, for qualitative discussions about the nature of bonding interactions, such as those presented here, one expects the results to be rather insensitive to the details of assumed cluster sizes and geometries. This statement is made on the basis of numerous cluster studies of other problems which have appeared in the literature. With this caveat stated, it should be apparent, nonetheless, that such theoretical results should be very useful in focusing future investigations.

TABLE I. Effective magneton numbers.

Theory		Experiment[a]	
Cluster	n_B	Alloy	n_B
Ni_2Fe_2	1.65	$Ni_{50}Fe_{50}$	1.65
Ni_2Fe_2B	1.38	$Ni_{40}Fe_{40}B_{20}$	1.31
	1.71[b]		
	0.83[c]		
Ni_2Fe_2P	0.83	$Ni_{40}Fe_{40}P_{20}$	1.08

[a] See Refs. 12 and 13.
[b] Value obtained with nonintegral occupation solution.
[c] Value obtained for short metal–metalloid distance (1.53 Å).

In order to ascertain whether there are specific interactions between metal atoms and metalloid atoms, an analysis of bonding charge densities between the metalloid atom and the metal atoms should be particularly useful. The total charge density for a system is given by

$$\rho_T(\vec{r}) = \sum_j n_j \phi_j^*(\vec{r}) \phi_j(\vec{r}) , \tag{1}$$

where the $\phi_j(\vec{r})$ are the molecular orbitals of the system, the n_j are occupation numbers, and $\rho_T(\vec{r})$ is the total charge density. However, as there are relatively few molecular orbitals which describe the metal-metalloid interaction, it is convenient to consider a partial charge density or bonding charge density defined as

$$\rho_M(\vec{r}) = \sum_{j(M)} n_j \phi_j^*(\vec{r}) \phi_j(\vec{r}) , \tag{2}$$

where the sum is over only those orbitals which contain appreciable (> 5%) metalloid (*M*) character.

For the case of the Ni_2Fe_2B cluster, the orbitals $1a_1^\uparrow$, $1a_1^\downarrow$, $5a_1^\uparrow$, $4b_1^\uparrow$, $3b_2^\uparrow$, $1b_2^\downarrow$, $2a_1^\downarrow$, and $1b_1^\downarrow$ will contribute to the bonding charge density ρ_B. If this charge density is plotted in the *yz* plane (see Fig. 1), which will be denoted as ρ_B^{yz}, it should show the metalloid bonding to the Ni atoms. On the other hand, if it is plotted in the *xz* plane the charge density ρ_B^{xz} should show the metalloid bonding to the Fe atoms. In order to see if there is a preferential interaction, a difference density $\Delta\rho_B$ can be obtained by aligning the metal atoms from the two planes such that they coincide. Thus $\Delta\rho_B$ is defined as $\Delta\rho_B = \rho_B^{yz} - \rho_B^{xz}$ once the metal atoms have been properly aligned. If there is a preferential interaction between the B atom and the Ni atoms, positive contour lines of $\Delta\rho_B$ should surround the B atom as ρ_B^{yz} is in the Ni_2B plane, whereas negative contour lines of $\Delta\rho_B$ should surround the B atom if the preferential interaction is between B and the Fe atoms (ρ_B^{xz} is in the Fe_2B plane). A contour plot of $\Delta\rho_B$ for the Ni_2Fe_2B cluster is shown in Fig. 7. The contours around the B atom are positive indicating a preferential B-Ni interaction.

The same procedure is used to compute $\Delta\rho_P$ for the Ni_2Fe_2P cluster. For this case the partial summation defined in Eq. (2) involves only the $1a_1^\uparrow$, $1a_1^\downarrow$, $1b_2^\uparrow$, $2a_1^\downarrow$, and $1b_1^\downarrow$ orbitals. The contour plot of $\Delta\rho_P$ is shown in Fig. 8. From this plot it can be seen that the contour values around the P atom are negative. This suggests a preferential P-Fe interaction. However, in comparison to the Ni_2Fe_2B situation, where positive contours of $\Delta\rho_B$ surround both the B and metal sites, for the

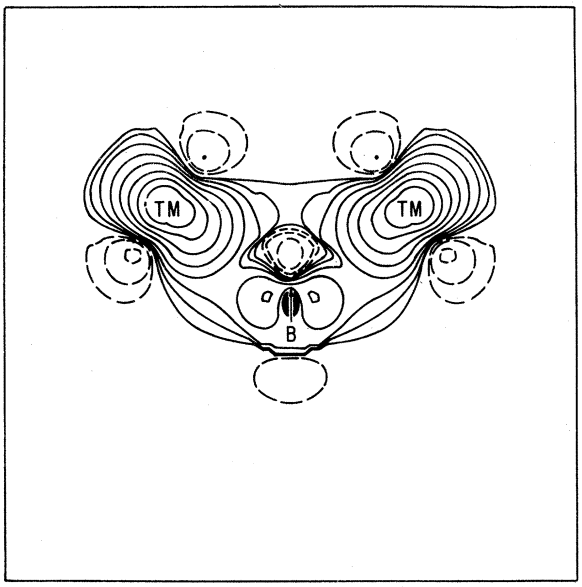

FIG. 7. Plot of difference bonding charge density $\Delta\rho_B$ for Ni_2Fe_2B. See text for discussion. Positive contours about B and transition-metal (TM) sites show that there is a preferential Ni-B bonding interaction. The charge-density contour values start at 0.001 a.u. and double for each successive contour value.

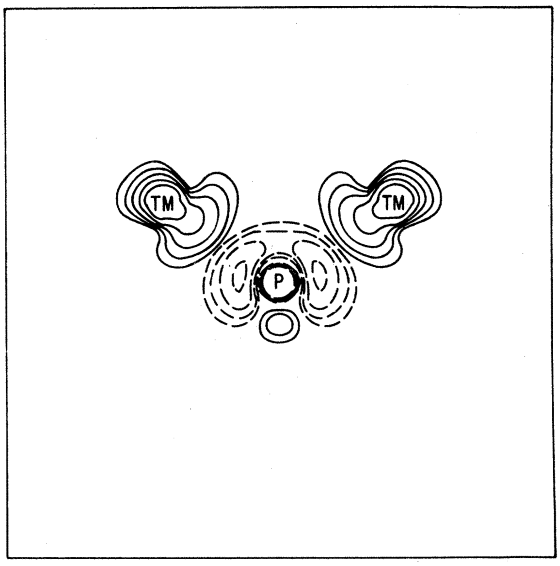

FIG. 8. Plot of difference bonding charge density $\Delta\rho_P$ for Ni_2Fe_2P. Negative contours about P suggest a preferential Fe-P interaction. See text for discussion. Contour values are the same as in Fig. 7.

Ni_2Fe_2P situation the negative contours surround only the P atom. A closer analysis of this latter case shows that the charge densities in the Fe_2P and Ni_2P planes practically cancel each other for the $1a_1^{\uparrow}$, $1a_1^{\downarrow}$, and $2a_1^{\downarrow}$ orbitals. This leaves only a difference of the $1b_2^{\uparrow}$ and $1b_1^{\downarrow}$ orbitals as being the dominant contribution to the $\Delta\rho_P$ of Fig. 8. The $1b_2^{\uparrow}$ orbital lies in the yz plane (Ni_2P plane), whereas the $1b_1^{\downarrow}$ orbital lies in the xz plane (Fe_2P plane). The fact that the former orbital has less P character than the latter orbital, whereas the former orbital has more Ni character than the latter orbital has Fe character, leads to the form of $\Delta\rho_P$ in Fig. 8.

Thus the evidence for a specific Fe-P interaction is not as clear-cut as one might like for the Ni_2Fe_2P cluster as a consequence of too few orbitals being involved. This is a case where results on a larger cluster would clearly be desirable. However, in order to provide additional information on Fe-P interactions and stay within the framework of tetrahedral clusters, two additional calculations have been performed. These calculations are for the Ni_4P and Fe_4P tetrahedral clusters, using the same interatomic distances as for the previous clusters. In this instance a $\Delta\rho_P$ can be defined as $\rho_P(Ni_4P)-\rho_P(Fe_4P)$. If $\Delta\rho_P$ is plotted in the same plane as done previously, the contour plot of Fig. 9 is obtained. This clearly shows negative contours connecting the P atom with metal sites, a consequence of substantial Fe-P preferential interaction. For these two clusters more orbitals contribute to the determination of $\Delta\rho_P$ than those for the Ni_2Fe_2P cluster,

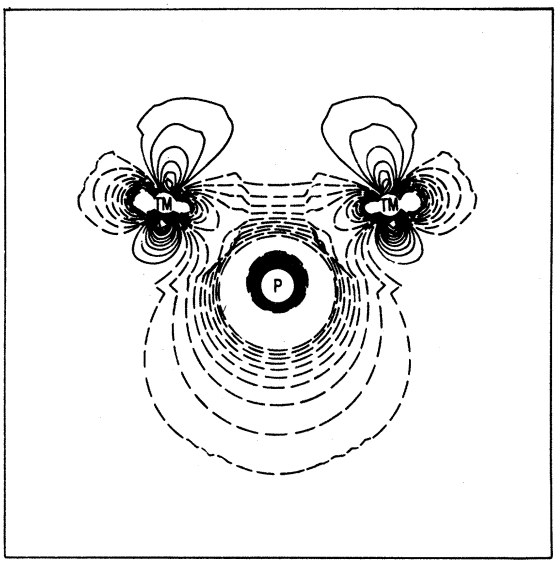

FIG. 9. Plot of difference bonding charge density $\Delta\rho_P$ obtained by subtracting bonding charge density of Fe_4P from the bonding charge density of Ni_4P. See text. The negative contours about P and the transition-metal (TM) sites show a preferential Fe-P interaction. The contour values are the same as in Fig. 7.

and hence the problems encountered for the latter cluster do not arise.

Recently experimental evidence for some sort of chemical ordering between Ni and B has been found for $Ni_xFe_yB_z$ alloys.[14] It was found from differential scanning calorimetry (DSC) that for the $Fe_{100-x}B_x$ alloy series, the temperature of maximum heat evolution (T_p), the temperature of initiation of crystallization (T_x), and the glass transition temperature (T_g) all increased with increasing B content. However, for the two series of alloys $(Fe_{1-x}Ni_x)_{80}B_{20}$ and $(Fe_{0.5}Ni_{0.5})_{100-x}B_x$ it was found that all three temperatures decreased as a function of increased Ni and B content, respectively. It was concluded from these results that a chemical ordering occurs between the nickel and boron atoms which decreases the viscosity and hence the energy for hole formation. Thus with increasing boron and nickel content T_g and T_x are decreased.

The present theoretical results suggest that the nature of this chemical ordering is due to a preferential bonding interaction between boron and nickel atoms. Furthermore, the present results suggest that a preferential iron-phosphorus interaction also exists. Similar DSC experiments for a different set of alloys are now being carried out to see if there is corresponding evidence for an iron-phosphorus chemical ordering.[15]

Recent extended x-ray-absorption fine-structure (EXAFS) experiments[16] on $Ni_{40}Fe_{40}B_{20}$ and $Ni_{40}Fe_{40}P_{20}$ alloys have examined the fractional change in thermal disorder with respect to a low-temperature state. It was concluded from the results for the $Ni_{40}Fe_{40}B_{20}$ glass that there was a preferential coordination of the boron with nickel which forms a more tightly bound shell around the nickel atoms such that a dynamic coupling of the nickel atoms with their local environment takes place. For the $Ni_{40}Fe_{40}P_{20}$ alloy, a similar analysis led to the conclusion that there was a preferential coordination of P with iron. Although these results provide rather indirect evidence for preferential interactions, a more detailed analysis of the EXAFS data now underway[17] should provide more direct microscopic information.

Although the theoretical results thus far are restricted to rather small clusters, they do demonstrate the utility of such cluster investigations. Furthermore, the implications of such calculations transcend the problem of amorphous alloys. They are of potential value in discussing impurities which segregate to grain boundaries as well as other important problems in metals physics. Such implications will be discussed in forthcoming publications.

ACKNOWLEDGMENT

This work was partially supported by the U.S. Department of Energy under Contract No. DE-AC02-79ER-10382.

APPENDIX

In order to carry out an $X\alpha$-scattered-wave calculation one must specify the following quantities: the coordinates of the atoms, the sphere sizes which characterize the muffin-tin potential, the partial-wave expansions on the various atoms, and the exchange factors or α values for the various atoms or regions of space. The coordinates can easily be obtained from the information on metal–metalloid distances for the clusters which are presented in the main text. For the other quantities, in the case of the metal–metalloid distance of 2.13 Å, the outer-sphere radius is 3.370 Å, the metal-sphere radii are 1.245 Å, and the metalloid-sphere radius is 0.880 Å; the partial-wave expansions have maximum l values of 4, 2, and 1 for the outer sphere, metal atoms, and metalloid atom, respectively; the atomic α values are those tabulated by Schwarz[18] and denoted by him as α_{HF}; and the α values in the inner- and outer-sphere regions are weighted averages.

[1]M. Matsuura, T. Nomoto, F. Itoh, and K. Suzuki, Solid State Commun. 33, 895 (1980).
[2]D. S. Boudreaux, Phys. Rev. B 18, 4039 (1978).
[3]W. L. Johnson and A. R. Williams, Phys. Rev. B 20, 1640 (1979).
[4]R. P. Messmer and G. D. Watkins, Phys. Rev. B 7, 2568 (1973).
[5]R. P. Messmer and D. R. Salahub, Phys. Rev. B 16, 3415 (1977).
[6]K. H. Johnson, D. D. Vvedensky, and R. P. Messmer, Phys. Rev. B 19, 1519 (1979).
[7]C. L. Briant and R. P. Messmer, Philos. Mag. B 42, 569 (1980).
[8]S. Rundquist, Acta. Chem. Scand. 61, 1 (1962); 61, 242 (1962); 61, 992 (1962).
[9]J. C. Slater and K. H. Johnson, Phys. Rev. B 5, 844 (1972); K. H. Johnson and F. C. Smith, Jr., *ibid.* 5, 831 (1972).
[10]R. P. Messmer, S. K. Knudson, K. H. Johnson, J. B. Diamond, and C. Y. Yang, Phys. Rev. B 13, 1396 (1976).
[11]T. E. Fischer, S. R. Kelemen, K. P. Wang, and K. H. Johnson, Phys. Rev. B 20, 3124 (1979).
[12]E. Kneller, *Ferromagnetismus* (Springer, Berlin,

1962), p. 148.
[13]J. J. Becker, F. E. Luborsky, and J. L. Walter, IEEE Trans. Magn. MAG-13, 988 (1977).
[14]J. L. Walter, Mater. Sci. Eng. 39, 95 (1979).
[15]J. L. Walter, private communication.
[16]J. Wong, F. W. Lytle, R. B. Greegor, H. H. Liebermann, J. L. Walter, and F. E. Luborsky, in *Rapidly Quenched Metals III*, edited by B. Cantor (The Metal Society, London, 1978), Vol. 2, p. 345.
[17]J. Wong, private communication.
[18]K. Schwarz, Phys. Rev. B 5, 2466 (1972).